HHS Public Access

Author manuscript

Brain Topogr. Author manuscript; available in PMC 2022 July 01.

Published in final edited form as:

Brain Topogr. 2021 July ; 34(4): 415–429. doi:10.1007/s10548-021-00845-1.

Simultaneous recording of motor evoked potentials in hand, wrist and arm muscles to assess corticospinal divergence

Stacey L. DeJong, PhD[1], **Jayden A. Bisson**[1], **Warren G. Darling, PhD**[2], **Richard K. Shields, PhD**[1]

[1]Department of Physical Therapy and Rehabilitation Science, Carver College of Medicine, University of Iowa, Iowa City, IA, USA

[2]Department of Health and Human Physiology, University of Iowa, Iowa City, IA, USA

Abstract

Objective: To further develop methods to assess corticospinal divergence and muscle coupling using transcranial magnetic stimulation (TMS).

Methods: Ten healthy right-handed adults participated (7 females, age 34.0 ± 12.9 years). Monophasic single pulses were delivered to 14 sites over the right primary motor cortex at 40, 60, 80 and 100% of maximum stimulator output (MSO), using MRI-based neuronavigation. Motor evoked potentials (MEPs) were recorded simultaneously from 9 muscles of the contralateral hand, wrist and arm. For each intensity, corticospinal divergence was quantified by the average number of muscles that responded to TMS per cortical site, coactivation across muscle pairs as reflected by overlap of cortical representations, and correlation of MEP amplitudes across muscle pairs.

Results: TMS to each muscle's most responsive site elicited submaximal MEPs in most other muscles. The number of responsive muscles per cortical site and the extent of coactivation increased with increasing intensity (ANOVA, $p < 0.001$). In contrast, correlations of MEP amplitudes did not differ across the 60, 80 and 100% MSO intensities (ANOVA, $p = 0.34$), but did differ across muscle pairs (ANOVA, $p < 0.001$). Post hoc analysis identified 4 sets of muscle pairs (Tukey homogenous subsets, $p < 0.05$). Correlations were highest for pairs involving two hand muscles and lowest for pairs that included an upper arm muscle.

Conclusions: Correlation of MEP amplitudes may quantify varying levels of muscle coupling. In future studies, this approach may be a biomarker to reveal altered coupling induced by neural injury, neural repair and/or motor learning.

Corresponding author: Dr. Stacey L. DeJong stacey-dejong@uiowa.edu.

Ethical approval: All procedures were in accordance with the ethical standards of the University of Iowa Human Subjects Institutional Review Board and with the 1964 Helsinki declaration and its later amendments.

Conflict of Interest: The authors declare that they have no conflict of interest.

Keywords

transcranial magnetic stimulation; motor evoked potential; cortical mapping; coactivation; synergy; muscle coupling

Introduction:

As early as the 1870's, scientists began to recognize that neurons in the primary motor cortex contribute to limb movement by activating muscles in task-related combinations, rather than controlling each muscle individually (Fritsch and Hitzig 1870; Ferrier 1873). Since that time, a contemporary understanding of corticospinal organization has evolved, based on anatomical, neurophysiological and behavioral studies in animals and humans, and has illuminated the neural underpinnings of muscle coactivation (Omrani et al. 2017). While Penfield's somatotopic representation of body regions on the precentral gyrus generally holds true (Penfield and Rasmussen 1950), additional complexity has been revealed on a finer scale. Muscles are represented in a mosaic pattern, extensively overlapping and intermingling with the representations of other muscles (Schieber and Hibbard 1993; Nudo et al. 1996; Sanes and Schieber 2001; Devanne et al. 2006). For each muscle, excitability varies across the spatial extent of the cortical representation, such that motor evoked potentials (MEPs) with relatively large amplitude can be elicited at multiple discrete stimulation sites (Schneider et al. 2001; Masse-Alarie et al. 2017). Muscle representations are chained together by horizontal collateral projections from corticospinal axons, which are studded with synaptic boutons all along their course and establish extensive reciprocal connectivity between clusters of cortical neurons (Huntley and Jones 1991; Capaday 2004; Card and Gharbawie 2020). Additionally, axonal branching in the spinal cord distributes the corticospinal projection to the motor neuron pools of multiple muscles (Shinoda et al. 1981; Cheney and Fetz 1985).

Modern theories of motor control contend that these mechanisms of corticospinal divergence establish the neural substrate needed for a vast repertoire of movement options (Ethier et al. 2006; McMorland et al. 2015; Overduin et al. 2015; Rana et al. 2015). It is well accepted that the motor cortex controls movements, not individual muscles, and that transient associations within the diffuse neural circuitry rapidly form and turn off task-specific motor synergies (Gentner and Classen 2006; Barchiesi and Cattaneo 2013). During performance of a motor task, groups of muscles, referred to as synergies or motor modules, may be activated together with time-varying intensity, in flexible combinations with other motor modules, to generate the necessary muscle activation pattern (Bizzi et al. 2008; Safavynia et al. 2011; Bizzi and Cheung 2013). This view has been supported by the use of non-negative matrix factorization to analyze muscle activation patterns during a variety of movements and postural control tasks (Neptune et al. 2009; Torres-Oviedo and Ting 2010; Roh et al. 2012).

In recent decades, transcranial magnetic stimulation (TMS) has become a widely used tool to more directly examine corticospinal output noninvasively in humans. Despite its low spatial resolution as compared to invasive methods, cortical mapping with TMS is a useful neurophysiological assessment. For a given muscle, the location and spatial area

of its cortical representation can be identified, and excitability can be quantified with variables including the resting and active motor thresholds, recruitment curves, MEP amplitudes and map volumes (Groppa et al. 2012). Extensive literature over the past several decades demonstrates the value of cortical mapping to identify distinct, yet overlapping representations of closely associated muscles (Wilson et al. 1993; Devanne et al. 2006; Raffin et al. 2015), to quantify the extent of corticospinal connectivity remaining to a given muscle after a lesion (Trompetto et al. 2000; Bembenek et al. 2012), and to track changes that result from use-dependent and/or lesion-induced neural adaptation (Byrnes et al. 2001; Thickbroom et al. 2004; Tyc et al. 2005; Tyc et al. 2012; Buick et al. 2016).

Despite these contributions, the vast majority of TMS mapping studies to date have focused on the convergent properties of the corticospinal pathway, in which neurons throughout an area of cortex converge onto an individual muscle. In contrast, few have explored the divergent properties, in which stimulation of an individual cortical site results in the coactivation of multiple muscles, perhaps reflecting the neural linkage of muscles into motor modules that form the building blocks of movement.

Two notable exceptions have been reported. Melgari et al. (Melgari et al. 2008) simultaneously recorded EMG from 12 upper limb muscles while stimulating cortical sites in an 11 × 11 cm grid, centered around the hotspot of the opponens pollicis muscle. For each pair of muscles, the extent of map overlap was quantified as a measure of muscle coactivation, and the correlation of MEP amplitudes was determined. The authors described the correlation measure as an index of the intensity and direction of the coactivation, and suggested that it gives “evidence of the motor cortex representation of muscle synergies”. Results revealed differences in coactivation and correlation across muscle pairs, consistent with functional use of the hand and arm. Muscle pairs that included two hand muscles, a hand muscle plus a forearm muscle, or two forearm muscles consistently showed high coactivation and correlation, as compared to muscle pairs that included at least one upper arm muscle. In the Melgari study, however, a single stimulus intensity was selected (resting motor threshold of the opponens pollicis plus 10% of the maximum stimulator output (%MSO)). The authors acknowledged that thresholds vary across muscles, typically in a distal to proximal gradient, with distal muscles demonstrating the lowest thresholds. To avoid excessive ‘cortical spread’ of the stimulus, a relatively low stimulus intensity was used and may have limited the ability to assess coactivation and correlation, especially for the more proximal muscles.

Mathew et al. (Mathew et al. 2016) explored coactivation patterns by stimulating a single cortical site (the extensor carpi ulnaris hotspot) at varying intensities while simultaneously recording responses from three highly synergistic wrist extensor muscles (extensor carpiulnaris (ECU), extensor carpi radialis (ECR), and extensor digitorum communis (EDC)). The cortical representation was also assessed for each muscle. Greater similarity in stimulus-response curves and greater overlap of cortical representations indicated that the ECU/EDC muscle pair was more strongly functionally coupled, compared to the other muscle pairs (ECU/ECR and EDC/ECR), especially in the left hemisphere.

Findings from the two studies above suggest an expanded purpose of neurophysiological assessment using TMS. Beyond the excitability measures generated by traditional cortical mapping procedures, alternative methods and analyses may quantify the extent of corticospinal divergence from focal cortical sites to sets of muscle targets. This may offer insight into functional muscle coupling in healthy people and in those with movement impairments after neural injury. For example, abnormal muscle coactivation patterns often constrain upper limb movements into flexion-dominated synergies after stroke, limiting functional use of the arm and hand, and restricting participation in daily life. Objective, quantitative assessments of abnormal muscle synergies are lacking in both clinical and research environments.

The purpose of this study was to further develop methods to evaluate corticospinal divergence and functional muscle coupling using TMS. We identified sites throughout the primary motor cortex using neuronavigation, stimulated each site at a range of stimulus intensities, and recorded MEPs from nine muscles of the contralateral hand, forearm and upper arm simultaneously. We also examined the extent to which stimulus intensity affected the number of muscles that responded to stimulation at each site, the overlap of cortical representations within primary motor cortex, and the correlation of MEP amplitudes across muscle pairs.

Materials and Methods:

Subjects

Healthy right-handed adults were recruited via email advertisement at an academic medical center. Potential participants were excluded if they had a current or previous neurological diagnosis, a musculoskeletal condition affecting movement of the upper limb on either side, or a contraindication to TMS (Rossi et al. 2011) or magnetic resonance imaging (MRI). The study was approved by the University of Iowa Human Subjects Institutional Review Board. Informed consent was obtained from all individual participants included in the study.

Ten healthy right-handed adults participated, including 7 females and 3 males. Ages ranged from 22 to 56 years (mean 34.0, SD 12.9 years). Body mass index ranged from 20 to 35 (mean 27.4, SD 5.2).

Neuronavigated TMS Procedures:

Stimulation sites over the right primary motor cortex were identified and targeted using a frameless stereotaxic neuronavigation system (Brainsight, Rogue Research Inc., Montreal, QC, Canada). Each participant first underwent magnetic resonance imaging of the brain in a 3T Siemens Trio Tim scanner. Each participant's T1-weighted anatomical image was loaded into the Brainsight software, and a 7 × 2 grid pattern was aligned over the right precentral gyrus (Figure 1). The 1 cm distance between stimulation sites was chosen because the geometry of the TMS coil yielded peak magnetic field intensity in an area approximately 1 cm in diameter, and to allow comparison to previous cortical mapping studies, most of which also used a grid with 1 cm spacing (Wassermann et al. 1992; Wilson et al. 1993; Devanne et al. 2006; Kleim et al. 2007). In addition, since the smallest cortical

representations of proximal upper limb muscles are approximately 6 cm^2 (Wassermann et al. 1992), the spatial frequency of 1 site per cm exceeds the necessary sampling frequency indicated by the Shannon-Nyquist anti-aliasing principle (Cattaneo 2018). The grid was carefully placed, such that the 2 columns were parallel to and centered rostrocaudally over the precentral gyrus, and the middle row was aligned mediolaterally with the anatomical landmark known as the 'hand knob' (Yousry et al. 1997; Ahdab et al. 2016; Vigano et al. 2019). Curvature of the grid was adjusted to optimize placement of the stimulation targets on the cortical surface. During each TMS session, the Brainsight optical tracking system was used to co-register the participant's head, the TMS coil, and the pre-loaded MR image, allowing for precise and repeatable targeting of each stimulation site (Kleim et al. 2007).

Single-pulse monophasic TMS was delivered using a MagVenture MagPro X100 stimulator with MagOption and a butterfly coil with an outer diameter of 75 mm (MagVenture MCF-B65) (MagVenture, Inc., Alpharetta, GA). Throughout all sessions, the stimulator was used in 'Power mode', which increased the peak stimulus intensity by approximately 40%. Before each pulse was delivered, the coil was carefully aligned with the target site, using Brainsight to assure less than 0.2 mm error in the rostrocaudal and mediolateral location, and less than 2 degrees error in the orientation tangential to the cortical surface. The coil was rotated to align the handle posterolaterally and perpendicular to the pre-positioned grid over the precentral gyrus. The 'Reverse' current direction was selected in the MagVenture system, producing an anteromedial-to-posterolateral current direction at the center of the coil, and therefore a posterolateral-to-anteromedial direction of induced currents in the cortex. Each stimulus was a single monophasic pulse of approximately 98 μs duration. Consecutive stimuli were separated by an interstimulus interval that varied randomly between 4 and 10 seconds.

During all TMS procedures, MEPs were recorded from nine contralateral (left) upper limb muscles simultaneously, using a wireless surface electromyography (EMG) system (Trigno, Delsys, Inc., Natick, MA). After the skin over each target muscle was cleaned with an alcohol wipe, standard-sized Trigno sensors were applied over the muscle belly of the abductor pollicis brevis (APB), flexor carpi radialis (FCR), flexor digitorum superficialis (FDS), extensor carpi radialis longus (ECR), extensor digitorum communis (EDC), biceps brachii short head (BB), triceps brachii lateral head (TB), and lateral deltoid (LD). A Trigno Mini sensor was applied over the muscle belly of the first dorsal interosseous (FDI). All sensors included the Delsys parallel silver bar technology, a fixed inter-electrode distance of 10 mm, and a bandwidth of 20-450 Hz. Wireless (digital) EMG signal transmission minimized electromagnetic interference, resulting in a low noise level of 5-10 μV peak-to-peak. A 300 ms epoch of EMG data corresponding to each TMS pulse was collected through a custom-written Lab VIEW program (National Instruments, Austin, TX), initiated by a trigger output from the MagVenture system 100 ms before each TMS stimulus was delivered. Data were sampled at 2000 Hz and were saved to files for subsequent analysis offline. Immediately after each stimulus, EMG signals and peak-to-peak MEP amplitudes were displayed on a monitor, to allow the examiners to verify a resting state of background EMG in each muscle, and to view MEP amplitudes in nearly real time.

To maintain consistent symmetrical posture and to facilitate relaxation, the participant was seated in a slightly reclined barber chair with head and neck support, and each arm was positioned using a Versaform vacuum molded pillow (Performance Health, Warrenville, IL). Each arm was supported in approximately 20° of shoulder abduction and flexion, 80° of elbow flexion, neutral forearm pronation/supination, neutral wrist flexion/extension, and a relaxed hand posture with the fingers flexed (Figure 2). Synergies evoked with TMS are known to be task dependent, and in this study the task was to remain at rest. Participants were instructed to keep their muscles relaxed and to remain alert with eyes open. All sessions were conducted in a quiet room, and conversation was limited to essential communication regarding the procedures.

During a single data collection session, 5 consecutive single pulses were delivered to each of the 14 stimulation sites at 40, 60, 80 and 100 %MSO). Throughout the session, EMG recordings were carefully monitored to verify relaxation. If EMG activity was evident prior to a TMS pulse, the trial was discarded, and an additional trial was recorded, to ensure 5 usable repetitions for each intensity at each site. All grid sites were stimulated at one intensity before advancing to the next intensity.

Data Analysis:

MEP data were analyzed using custom-written MATLAB software (The MathWorks, Inc., Natick, MA). All trials were screened to verify a relaxed state prior to stimulation. Trials were discarded if the EMG signal for any of the 9 muscles exceeded 30 μV during the pre-stimulus phase. Since background EMG was also monitored during the TMS session, this eliminated less than 1% of all recorded trials. On a trial by trial basis, peak-to-peak EMG amplitudes were determined for each muscle in the time window 10-50 ms following the TMS pulse, and responses greater than 50 μV were retained for further analysis (Figure 3). Average MEP amplitudes were determined for each stimulus intensity at each stimulation site by averaging across the 5 trials. To allow comparison across muscles, average MEP amplitudes were expressed as a percentage of the largest average MEP amplitude obtained for the given muscle at any stimulation site at any intensity (i.e. normalized to the maximum MEP).

Stimulus-response relationships were examined for all 9 muscles at each of the 14 cortical sites, by plotting the normalized MEP amplitudes across stimulus intensities, and calculating the area under the stimulus-response plot. For each muscle, the most responsive site was operationally defined as the stimulation site at which TMS produced the largest average MEP amplitude in the given muscle. Stimulus-response plots were created, showing responses of all 9 muscles when TMS was delivered at each muscle's most responsive site (Figure 4).

Divergence from the primary motor cortex to upper limb muscles was quantified in three ways. First, for each stimulus intensity at each cortical site, we determined how many of the 9 muscles responded to TMS with an average MEP amplitude greater than 50 μV. The average number of responsive muscles per cortical site was calculated for each participant, by averaging across the 14 cortical sites. The effect of stimulus intensity on the average

number of responsive muscles was examined with a 1-way repeated-measures ANOVA, followed by Tukey post-hoc comparisons where indicated.

Divergence was also quantified by determining the extent of coactivation across muscle pairs. As described by Melgari et al. (Melgari et al. 2008), coactivation was defined as the percentage of overlapping cortical sites for the two muscles in a pair. For each muscle pair, the number of grid sites where TMS elicited an average MEP greater than 50 μV in both muscles was expressed as a percentage of the total number of grid sites where TMS elicited an average MEP greater than 50 μV in at least one of the two muscles. Data corresponding to the lowest stimulus intensity were excluded from this analysis, since TMS at 40% MSO yielded only one MEP at one site in one participant. In addition, muscle pairs that included TB or LD were excluded, because few responses were observed in those muscles. Effects of stimulus intensity and muscle pair on coactivation were examined using 2-way repeated-measures ANOVA, treating both intensity and muscle pair as within-subjects factors. Significant effects were identified using Tukey post-hoc comparisons where indicated.

Notably, the two measures of divergence described above both treat MEPs as binary phenomena (present if the average MEP is ≥ 50 μV, otherwise absent), and do not account for variation in the amplitude of responses to TMS. In contrast, correlation of MEP amplitudes between two muscles may provide insight into the intensity and direction of their coactivation, and may signify muscle synergy representations in the motor cortex (Melgari et al. 2008). Therefore, we also quantified divergence using the correlational method described by Melgari et al. (2008), for each of the 36 possible muscle pairs. For each of the 4 stimulus intensities, a data matrix was prepared for each participant, containing peak-to-peak amplitudes for each stimulus delivered at that intensity. Since 5 stimuli were delivered at 14 stimulation sites, the table for each participant consisted of 70 rows, with 9 columns corresponding to the 9 muscles. As described by Melgari et al. (2008), log transformation was applied to the peak-to-peak MEP amplitudes, to achieve a normal distribution. Then Pearson correlation coefficients of log-transformed peak-to-peak amplitudes were calculated for each muscle pair, and Fisher's transformation was applied to the Pearson correlation coefficients ($rPF = 0.5*\ln((1-r)/(1+r))$), resulting in a normally distributed z-score measure of correlation. Effects of stimulus intensity and muscle pair on correlation were examined using 2-way repeated-measures ANOVA, treating both intensity and muscle pair as within-subjects factors. Significant effects were identified using Tukey post-hoc comparisons where indicated.

Lastly, the stimulation sites were grouped into 4 clusters, to determine whether the coactivation and correlation variables differed across anterior versus posterior sites, and across medial versus lateral sites. The anterior cluster included sites numbered 2, 4, 6, 8, 10 and 12. The posterior cluster included sites numbered 1, 3, 5, 7, 9 and 11. Sites numbered 1 through 6 formed the medial group, and sites numbered 7 through 12 formed the lateral group. For each stimulus intensity, differences in co-activation and correlation across clusters were determined using 2-way repeated measures ANOVA, treating cluster and muscle pair as within-subjects factors.

Results:

Results demonstrate simultaneous responses in multiple upper limb muscles, resulting from TMS delivered at 40, 60, 80 and 100% MSO at sites throughout the primary motor cortex. Examples of raw EMG recordings show that the patterns of responses varied across participants and across cortical sites (Figure 3). Consistent coactivation patterns and increasing MEP amplitudes were sometimes observed as stimulus intensity was increased at a single cortical site (Fig. 3A, B, C). At some sites, a large response was observed in only one muscle (Fig. 3D), or in two synergists (Fig. 3E), with minimal activation of any other muscles. Activation of a proximal muscle (BB), sometimes occurred at a relatively low stimulus intensity, without MEPs in any distal muscles (Fig. 3F). MEPs were sometimes observed in all 9 muscles, at a maximal or submaximal intensity (Fig. 3G). The presence of isolated large responses in a single muscle (e.g. Fig. 3D and F) suggests that crosstalk between EMG channels was minimal, as expected given relatively small inter-electrode distance of 10 mm. In addition, in most cases the muscles of interest were far enough apart that volumetric crosstalk would not be expected. For example, electrodes on the hand muscles were more than 20 cm away from electrodes on the wrist muscles. Even for closely spaced electrodes (e.g. FDI and APB), signals recorded from the two muscles were clearly distinguishable (e.g. Fig. 3D).

The area under the stimulus-response plot, which serves as an estimate of each muscle's relative excitability, is shown in Table 1 for each of the 14 stimulation sites and for each muscle's most responsive site. Since the data were not normally distributed, median values are reported. Additionally, the number of subjects who demonstrated an MEP in each muscle is reported for each site. Few MEPs were elicited at the sites that were most medial (sites 1 and 2) and most lateral (sites 13 and 14), indicating sufficient coverage of the upper limb representation within primary motor cortex.

High-intensity stimulation of the most responsive cortical site for one wrist or digit muscle typically produced MEPs in all of the other wrist and digit muscles tested (Figure 4). Median amplitudes of the other muscles' responses ranged from 47% to 91% of their maximum MEPs. The values given in Table 1 represent the area under the plot of normalized MEP amplitudes across stimulus intensities (% of maximum MEP multiplied by % MSO). Comparison of these values across muscles offers insight into the relative levels of excitability of the different muscles at each cortical site. Note that in some cases the most responsive site (defined as the site where TMS elicited the largest average MEP) did not correspond to the site with the largest area under the stimulus response plot.

As expected, the proximal muscles (biceps, triceps and deltoid) were less excitable, as compared to the wrist and digit muscles (Amassian et al. 1995; Devanne et al. 2002). For example, biceps brachii MEPs were elicited in 5 of the 10 participants, from a median of 7 cortical sites (range 5-10). Triceps brachii MEPs occurred in only 2 participants, at 8 cortical sites in one participant and 9 cortical sites in the other. Lateral deltoid MEPs occurred in only 3 participants, at 2, 5 and 9 cortical sites.

Results for the first measure of divergence (the number of muscles that responded to TMS, averaged across the 14 stimulation sites) are shown in Figure 5A. No MEPs were observed when TMS was delivered at 40% MSO, except in one participant at one site, where one muscle responded (the APB). On average, TMS at 60% MSO produced MEPs in 1.55 ± 1.25 muscles per cortical site (mean ± SD), TMS at 80% MSO produced MEPs in 2.53 ± 1.48 muscles per cortical site, and TMS at 100% MSO produced MEPs in 3.66 ± 1.60 muscles per cortical site. The number of muscles that responded increased significantly as stimulus intensity was increased (repeated-measures ANOVA, $F_{(3,27)} = 40.7$, $p < 0.001$, partial eta-squared = 0.82). The number of muscles at each intensity differed significantly from the number that responded at each other intensity ($p < 0.05$ for all Tukey post-hoc comparisons).

For the second measure of divergence (coactivation), 2-way repeated-measures ANOVA demonstrated a significant main effect of intensity, ($F_{(2,18)} = 25.9$, $p < 0.001$ partial eta-squared = 0.74) and a significant main effect of muscle pair ($F_{(20,18)} = 15.2$, $p < 0.001$ partial eta-squared = 0.63), with no significant interaction ($p = 0.43$) (Figure 6A). The ANOVA included 3 levels of stimulus intensity, and 21 muscle pairs. As shown in Figure 5B, coactivation (the percent of cortical sites where MEPs were elicited in both muscles) increased with increasing stimulus intensity, averaging 32.7 ± 29.5% at 60% MSO (mean ± SD), 46.6 ± 30.8% at 80% MSO, and 59.2 ± 23.4% at 100% MSO. Tukey post-hoc analyses showed significant differences across the 3 intensities ($p < 0.05$ for all pairwise comparisons).

The significant main effect of muscle pair on coactivation was further examined using Tukey homogenous subsets. Since there was no significant interaction between stimulus intensity and muscle pair, data were averaged across the 3 intensities, and post-hoc analysis using a one-way repeated-measures ANOVA was used to determine differences across muscle pairs (Figure 7A). This analysis identified three homogenous groups, within which the level of coactivation was not significantly different. For example, four muscle pairs showed relatively high levels of coactivation and were not statistically different from each other (FDI-APB, EDC-ECR, FDI-EDC, and APB-EDC). Except for the FDI-APB pair, all others in this group were also similar to all other muscle pairs involving hand-forearm and forearm-forearm combinations. In contrast, all muscle pairs involving a hand-upper arm or forearm-upper arm combination demonstrated lower levels of coactivation.

For the third measure of divergence (correlation of MEP amplitudes), 2-way repeated-measures ANOVA demonstrated a significant main effect of muscle pair, ($F_{(2,18)} = 8.2$, $p < 0.001$ partial eta-squared = 0.80), with no significant main effect of stimulus intensity ($p = 0.34$), and no significant interaction ($p = 0.43$) (Figures 5C and 6B). As described above for the coactivation variable, analysis of the correlation variable included 3 stimulus intensities and 21 muscle pairs, and the effect of muscle pair was further examined with a 1-way ANOVA of data averaged across stimulus intensities. This analysis identified four homogenous groups (Figure 7B). The FDI-APB and EDC-ECR pairs showed relatively high correlations of MEP amplitudes (rPF > 1.2, Pearson r > 0.83) and were not significantly different. The EDC-ECR muscle pair overlapped with a group that also included other forearm-forearm and hand-forearm muscle pairs with high correlation values (rPF = 0.91 –

1.1, Pearson r = 0.72 – 0.80) (FDS-FCR, FCR-ECR, FDI-EDC, FDI-ECR, and APB-EDC). In a third homogenous group, all hand-forearm and forearm-forearm combinations except EDC-ECR and FDS-FCR showed similar correlations (rPF = 0.83 – 1.09, Pearson r = 0.68 – 0.80). In contrast, all muscle pairs involving a hand-upper arm or forearm-upper arm combination demonstrated lower correlations of MEP amplitudes (rPF < 0.4, Pearson r < 0.38).

Analysis of coactivation across site clusters revealed a significant main effect of cluster at 60% MSO ($F_{(3,747)} = 10.31$, $p < 0.001$) and 100% MSO ($F_{(3,747)} = 8.14$, $p < 0.001$), with no significant interactions between cluster and muscle pair (Figure 8). Coactivation was greater in lateral sites compared to medial sites at the 60% and 100% MSO intensities (Tukey post-hoc, $p < 0.001$). Analysis of correlations of MEP amplitudes across site clusters revealed a significant main effect of cluster at 80% MSO ($F_{(3,747)} = 10.74$, $p < 0.001$) and 100% MSO ($F_{(3,747)} = 22.98$, $p < 0.001$), with no significant interactions between cluster and muscle pair (Figure 8). Correlations of MEP amplitudes were lower in lateral sites compared to medial sites at the 80% and 100% MSO intensities (Tukey post-hoc, $p < 0.001$). There were no significant differences in coactivation or correlation when comparing anterior sites to posterior sites.

Discussion:

The correlation measure distinguished four significantly different sets of muscle pairs, across which the extent of muscle coupling varied. In addition, the correlation measure was relatively unaffected by the intensity of TMS, in contrast to the other measures of corticospinal divergence that we examined (Figure 5). Muscles that are known to be activated together frequently during functional movements demonstrated the largest correlation values (e.g. FDI and APB used together during pinching and precision gripping; EDC and ECR used together during wrist extension), whereas muscles that are less likely to be used together had less strongly correlated MEPs (e.g. BB and EDC). These findings are consistent with those reported by Melgari et al. in the only similar study of MEP amplitude correlations which used a single stimulation intensity (Melgari et al. 2008). We have extended this finding to multiple stimulation intensities.

Results for the number of responsive muscles per cortical site and for the coactivation measure concur with several previous studies showing extensive overlap of cortical representations of upper limb muscles (Wassermann et al. 1992; Wilson et al. 1993; Devanne et al. 2006; Marconi et al. 2007; Melgari et al. 2008). Wasserman et al., for example, recorded cortical maps of two distal muscles and two proximal muscles simultaneously (APB, FCR, BB and deltoid), using a TMS intensity of 100% MSO. All four muscle representations were highly superimposed, yet distinguishable from each other by their thresholds, areal shapes, MEP amplitudes and the somatotopic arrangement of optimal sites (Wassermann et al. 1992). Devanne et al. (2006) later used more focal mapping methods to identify representations of the FDI, ECR and anterior deltoid. Each muscle was mapped separately, with a smaller, more focal TMS coil, a low level of voluntary activation in the target muscle, and lower stimulus intensities of 110-120% of the target muscle's active motor threshold. Despite this more focal mapping method, representations for all three

muscles overlapped. In addition, sharp demarcations were observed between map borders, indicating that the overlap was not due to stimulus spread alone. Rather, the overlap of muscle representations is now considered to be an important feature of cortical organization that underlies coordinated muscle activation (Capaday 2004; Devanne et al. 2006; Masse-Alarie et al. 2017).

Analysis of the coactivation and correlation variables in clusters of anterior, posterior, medial and lateral stimulation sites revealed differences across the medial versus lateral dimension. Compared to medial sites, lateral sites demonstrated greater coactivation (map overlap), which may be due to the lower thresholds observed in the more distal muscles, which are represented more laterally in the primary motor cortex. Additionally, lateral sites demonstrated lower correlations of MEP amplitudes than medial sites. This finding may reflect the more fractionated muscle activation patterns associated with dexterous fine motor movements executed by the more distal muscles.

In the current study, we focused on stimulation sites within the primary motor cortex using MRI-based neuronavigation, and expanded on traditional cortical mapping methods by recording stimulus-response relationships simultaneously in nine muscles of the upper limb. Data presented in Table 1 and Figure 4 provide a highly novel contribution to the literature, by indicating the extent and magnitude of coactivations induced by TMS to a single cortical site. For each hand and wrist muscle, stimulation at the optimal site also activated all other hand and wrist muscles, to varying submaximal extents. Similarly, when an MEP was elicited from the BB muscle at its optimal site, submaximal MEPs were also observed in all hand and wrist muscles.

In accordance with prior studies, our results also show that an increase in stimulation intensity increases the number of muscles that respond to TMS per cortical site, and the extent of coactivation (i.e. overlap) (Thickbroom et al. 1998; Kallioniemi and Julkunen 2016; van de Ruit and Grey 2016). This limits the usefulness of these measures for the assessment of corticospinal divergence. Because motor thresholds are lower in distal muscles than in proximal muscles (Wassermann et al. 1992), simultaneous mapping of many muscles at any single intensity will cause differential scaling across the individual muscle representations. Alternatively, mapping of each muscle at a given percentage of its motor threshold would necessarily have to be done individually for each muscle, limiting the feasibility of examining many muscle representations in a tolerable timeframe, while maintaining a stable neural state. Thus the MEP correlation measure may be the more suitable assessment, given that it is relatively unaffected by stimulus intensity. Maximal TMS intensity will exceed threshold in the largest number of muscles, allowing analysis of more muscle pairs.

Additional studies will be necessary to determine whether MEP correlations are sufficiently valid, reliable and meaningful as a method to quantify muscle coupling in healthy people and those with movement problems. For example, the measure may capture a different aspect of activity dependent neural plasticity in athletes, musicians and others with highly trained movement abilities, beyond the excitability changes that have been demonstrated in a few small studies (Tyc et al. 2005; Rosenkranz et al. 2007; Buick et al. 2016). In a

comparison of elite volleyball players versus runners, greater overlap of the deltoid and ECR representations was observed on the dominant side of volleyball players, as compared to their nondominant side and both sides of runners (Tyc et al. 2005). This suggests that motor learning and practice of coordinated movements may alter corticospinal connectivity, supporting common control and combined activation of the muscles involved. No prior studies have compared MEP correlations across muscle pairs in trained versus untrained individuals.

Similarly, the MEP correlation measure has the potential to quantify altered muscle coupling patterns in people with neurological movement impairments. After stroke, hemiparesis is often accompanied by abnormal muscle coactivation patterns that constrain upper limb movements into stereotypical flexion and extension synergies. For example, abnormal coupling of the shoulder abductors and elbow flexors has been well documented in stroke survivors (Dewald et al. 1995) and has been shown to reduce arm movement ability (Ellis et al. 2011). A TMS-based approach to quantify muscle coupling would allow these patterns to be more extensively studied, and might be useful for tracking neuroplastic changes after stroke and subsequent rehabilitation.

Further investigation of MEP correlation as a measure of muscle coupling should also include additional methodological development and refinement. In this initial study, stimulation was limited to 14 sites in the primary motor cortex, and the distance between sites was consistent across all participants despite individual differences in brain size. Each site was stimulated 5 times, at each of 4 intensities, coarse estimates of stimulus-response relationships were obtained using large increments of 20% MSO, and MEP amplitudes were expressed as a percentage of the MEP amplitude elicited with maximum-intensity TMS instead of the maximal M-wave for each muscle. In future studies, mapping at a single maximal intensity would enable more extensive sampling from a broader area of cortex, including premotor areas, without exceeding a reasonable session duration. Closer spacing of stimulation sites may also increase the likelihood of eliciting MEPs from proximal muscles (BB, TB and LD), and recording of M-waves could improve comparisons across muscles and across participants.

In summary, this study explored the use of TMS to quantify corticospinal divergence and upper limb muscle coupling in healthy adults. Correlation of MEP amplitudes across muscle pairs emerged as a potential novel assessment that can distinguish between different levels of muscle coupling, while being relatively unaffected by stimulus intensity. Further studies are needed to confirm these findings, to examine validity and reliability of the measure, and to explore potential applications in neural plasticity and rehabilitation research.

Acknowledgements:

This work was funded by the Comprehensive Opportunities for Rehabilitation Research Training (CORRT), a Multicenter Career Development Program for Physical and Occupational Therapists, National Institutes of Health grant number K12 HD055931, the University of Iowa Carver College of Medicine and the Department of Physical Therapy and Rehabilitation Science. MR scans were conducted on an MRI instrument funded by NIH 1S10OD025025-01. The authors acknowledge Lauren Werner for assistance with data collection.

Data Availability Statement:

The datasets generated during and/or analyzed during the current study are available from the corresponding author on reasonable request.

References:

Ahdab R, Ayache SS, Brugieres P, Farhat WH, Lefaucheur JP (2016) The Hand Motor Hotspot is not Always Located in the Hand Knob: A Neuronavigated Transcranial Magnetic Stimulation Study. Brain Topogr 29:590–597 doi: 10.1007/s10548-016-0486-2 [PubMed: 26980192]

Amassian VE, Cracco RQ, Maccabee PJ, Cracco JB, Henry K (1995) Some positive effects of transcranial magnetic stimulation. Adv Neurol 67:79–106 [PubMed: 8848984]

Barchiesi G, Cattaneo L (2013) Early and late motor responses to action observation. Soc Cogn Affect Neurosci 8:711–719 doi: 10.1093/scan/nss049 [PubMed: 22563004]

Bembenek JP, Kurczych K, Karli Nski M, Czlonkowska A (2012) The prognostic value of motor-evoked potentials in motor recovery and functional outcome after stroke - a systematic review of the literature. Funct Neurol 27:79–84 [PubMed: 23158578]

Bizzi E, Cheung VC (2013) The neural origin of muscle synergies. Front Comput Neurosci 7:51 doi: 10.3389/fncom.2013.00051 [PubMed: 23641212]

Bizzi E, Cheung VC, d'Avella A, Saltiel P, Tresch M (2008) Combining modules for movement. Brain Res Rev 57:125–133 doi: 10.1016/j.brainresrev.2007.08.004 [PubMed: 18029291]

Buick AR, Kennedy NC, Carson RG (2016) Characteristics of corticospinal projections to the intrinsic hand muscles in skilled harpists. Neurosci Lett 612:87–91 doi: 10.1016/j.neulet.2015.11.046 [PubMed: 26673887]

Byrnes ML, Thickbroom GW, Phillips BA, Mastaglia FL (2001) Long-term changes in motor cortical organisation after recovery from subcortical stroke. Brain Res 889:278–287 doi: 10.1016/s0006-8993(00)03089-4 [PubMed: 11166720]

Capaday C (2004) The integrated nature of motor cortical function. Neuroscientist 10:207–220 doi: 10.1177/107385403262109 [PubMed: 15155060]

Card NS, Gharbawie OA (2020) Principles of Intrinsic Motor Cortex Connectivity in Primates. J Neurosci 40:4348–4362 doi: 10.1523/JNEUROSCI.0003-20.2020 [PubMed: 32327531]

Cattaneo L (2018) Fancies and Fallacies of Spatial Sampling With Transcranial Magnetic Stimulation (TMS). Front Psychol 9:1171 doi: 10.3389/fpsyg.2018.01171 [PubMed: 30026721]

Cheney PD, Fetz EE (1985) Comparable patterns of muscle facilitation evoked by individual corticomotoneuronal (CM) cells and by single intracortical microstimuli in primates: evidence for functional groups of CM cells. J Neurophysiol 53:786–804 doi: 10.1152/jn.1985.53.3.786 [PubMed: 2984354]

Devanne H, Cassim F, Ethier C, Brizzi L, Thevenon A, Capaday C (2006) The comparable size and overlapping nature of upper limb distal and proximal muscle representations in the human motor cortex. Eur J Neurosci 23:2467–2476 doi: 10.1111/j.1460-9568.2006.04760.x [PubMed: 16706853]

Devanne H, Cohen LG, Kouchtir-Devanne N, Capaday C (2002) Integrated motor cortical control of task-related muscles during pointing in humans. J Neurophysiol 87:3006–3017 doi: 10.1152/jn.2002.87.6.3006 [PubMed: 12037204]

Dewald JP, Pope PS, Given JD, Buchanan TS, Rymer WZ (1995) Abnormal muscle coactivation patterns during isometric torque generation at the elbow and shoulder in hemiparetic subjects. Brain 118 (Pt 2):495–510 doi: 10.1093/brain/118.2.495 [PubMed: 7735890]

Ellis MD, Kottink AI, Prange GB, Rietman JS, Buurke JH, Dewald JP (2011) Quantifying loss of independent joint control in acute stroke with a robotic evaluation of reaching workspace. Conf Proc IEEE Eng Med Biol Soc 2011:8231–8234 doi: 10.1109/IEMBS.2011.6091940

Ethier C, Brizzi L, Darling WG, Capaday C (2006) Linear summation of cat motor cortex outputs. J Neurosci 26:5574–5581 doi: 10.1523/JNEUROSCI.5332-05.2006 [PubMed: 16707808]

Ferrier D (1873) Experimental Researches in Cerebral Physiology and Pathology. J Anat Physiol 8:152–155

Fritsch G, Hitzig E (1870) Electric excitability of the cerebrum (Uber die elektrische Erregbarkeit des Grosshirns). Arch Anat Physiol Wissen 37:300–332 doi: 10.1016/j.yebeh.2009.03.001

Gentner R, Classen J (2006) Modular organization of finger movements by the human central nervous system. Neuron 52:731–742 doi: 10.1016/j.neuron.2006.09.038 [PubMed: 17114055]

Groppa S, Oliviero A, Eisen A, et al. (2012) A practical guide to diagnostic transcranial magnetic stimulation: report of an IFCN committee. Clin Neurophysiol 123:858–882 doi: 10.1016/j.clinph.2012.01.010 [PubMed: 22349304]

Huntley GW, Jones EG (1991) Relationship of intrinsic connections to forelimb movement representations in monkey motor cortex: a correlative anatomic and physiological study. J Neurophysiol 66:390–413 doi: 10.1152/jn.1991.66.2.390 [PubMed: 1723093]

Kallioniemi E, Julkunen P (2016) Alternative Stimulation Intensities for Mapping Cortical Motor Area with Navigated TMS. Brain Topogr 29:395–404 doi: 10.1007/s10548-016-0470-x [PubMed: 26830768]

Kleim JA, Kleim ED, Cramer SC (2007) Systematic assessment of training-induced changes in corticospinal output to hand using frameless stereotaxic transcranial magnetic stimulation. Nat Protoc 2:1675–1684 doi: 10.1038/nprot.2007.206 [PubMed: 17641632]

Marconi B, Pecchioli C, Koch G, Caltagirone C (2007) Functional overlap between hand and forearm motor cortical representations during motor cognitive tasks. Clin Neurophysiol 118:1767–1775 doi: 10.1016/j.clinph.2007.04.028 [PubMed: 17576095]

Masse-Alarie H, Bergin MJG, Schneider C, Schabrun S, Hodges PW (2017) “Discrete peaks” of excitability and map overlap reveal task-specific organization of primary motor cortex for control of human forearm muscles. Hum Brain Mapp 38:6118–6132 doi: 10.1002/hbm.23816 [PubMed: 28921724]

Mathew J, Kubler A, Bauer R, Gharabaghi A (2016) Probing Corticospinal Recruitment Patterns and Functional Synergies with Transcranial Magnetic Stimulation. Front Cell Neurosci 10:175 doi: 10.3389/fncel.2016.00175 [PubMed: 27458344]

McMorland AJ, Runnalls KD, Byblow WD (2015) A neuroanatomical framework for upper limb synergies after stroke. Front Hum Neurosci 9:82 doi: 10.3389/fnhum.2015.00082 [PubMed: 25762917]

Melgari JM, Pasqualetti P, Pauri F, Rossini PM (2008) Muscles in “concert”: study of primary motor cortex upper limb functional topography. PLoS One 3:e3069 doi: 10.1371/journal.pone.0003069 [PubMed: 18728785]

Neptune RR, Clark DJ, Kautz SA (2009) Modular control of human walking: a simulation study. J Biomech 42:1282–1287 doi: 10.1016/j.jbiomech.2009.03.009 [PubMed: 19394023]

Nudo RJ, Milliken GW, Jenkins WM, Merzenich MM (1996) Use-dependent alterations of movement representations in primary motor cortex of adult squirrel monkeys. J Neurosci 16:785–807 [PubMed: 8551360]

Omrani M, Kaufman MT, Hatsopoulos NG, Cheney PD (2017) Perspectives on classical controversies about the motor cortex. J Neurophysiol 118:1828–1848 doi: 10.1152/jn.00795.2016 [PubMed: 28615340]

Overduin SA, d’Avella A, Roh J, Carmena JM, Bizzi E (2015) Representation of Muscle Synergies in the Primate Brain. J Neurosci 35:12615–12624 doi: 10.1523/JNEUROSCI.4302-14.2015 [PubMed: 26377453]

Penfield W, Rasmussen T (1950) The Cerebral Cortex of Man. MacMillan, New York

Raffin E, Pellegrino G, Di Lazzaro V, Thielscher A, Siebner HR (2015) Bringing transcranial mapping into shape: Sulcus-aligned mapping captures motor somatotopy in human primary motor hand area. Neuroimage 120:164–175 doi: 10.1016/j.neuroimage.2015.07.024 [PubMed: 26188259]

Rana M, Yani MS, Asavasopon S, Fisher BE, Kutch JJ (2015) Brain Connectivity Associated with Muscle Synergies in Humans. J Neurosci 35:14708–14716 doi: 10.1523/JNEUROSCI.1971-15.2015 [PubMed: 26538643]

Roh J, Rymer WZ, Beer RF (2012) Robustness of muscle synergies underlying three-dimensional force generation at the hand in healthy humans. J Neurophysiol 107:2123–2142 doi: 10.1152/jn.00173.2011 [PubMed: 22279190]

Rosenkranz K, Williamon A, Rothwell JC (2007) Motorcortical excitability and synaptic plasticity is enhanced in professional musicians. J Neurosci 27:5200–5206 doi: 10.1523/JNEUROSCI.0836-07.2007 [PubMed: 17494706]

Rossi S, Hallett M, Rossini PM, Pascual-Leone A (2011) Screening questionnaire before TMS: an update. Clin Neurophysiol 122:1686 doi: 10.1016/j.clinph.2010.12.037 [PubMed: 21227747]

Safavynia SA, Torres-Oviedo G, Ting LH (2011) Muscle Synergies: Implications for Clinical Evaluation and Rehabilitation of Movement. Top Spinal Cord Inj Rehabil 17:16–24 doi: 10.1310/sci1701-16 [PubMed: 21796239]

Sanes JN, Schieber MH (2001) Orderly somatotopy in primary motor cortex: does it exist? Neuroimage 13:968–974 doi: 10.1006/nimg.2000.0733 [PubMed: 11352603]

Schieber MH, Hibbard LS (1993) How somatotopic is the motor cortex hand area? Science 261:489–492 doi: 10.1126/science.8332915 [PubMed: 8332915]

Schneider C, Zytnicki D, Capaday C (2001) Quantitative evidence for multiple widespread representations of individual muscles in the cat motor cortex. Neurosci Lett 310:183–187 doi: 10.1016/s0304-3940(01)02105-x [PubMed: 11585597]

Shinoda Y, Yokota J, Futami T (1981) Divergent projection of individual corticospinal axons to motoneurons of multiple muscles in the monkey. Neurosci Lett 23:7–12 doi: 10.1016/0304-3940(81)90182-8 [PubMed: 6164967]

Thickbroom GW, Byrnes ML, Archer SA, Mastaglia FL (2004) Motor outcome after subcortical stroke correlates with the degree of cortical reorganization. Clin Neurophysiol 115:2144–2150 doi: 10.1016/j.clinph.2004.04.001 [PubMed: 15294217]

Thickbroom GW, Sammut R, Mastaglia FL (1998) Magnetic stimulation mapping of motor cortex: factors contributing to map area. Electroencephalogr Clin Neurophysiol 109:79–84 [PubMed: 9741796]

Torres-Oviedo G, Ting LH (2010) Subject-specific muscle synergies in human balance control are consistent across different biomechanical contexts. J Neurophysiol 103:3084–3098 doi: 10.1152/jn.00960.2009 [PubMed: 20393070]

Trompetto C, Assini A, Buccolieri A, Marchese R, Abbruzzese G (2000) Motor recovery following stroke: a transcranial magnetic stimulation study. Clin Neurophysiol 111:1860–1867 [PubMed: 11018503]

Tyc F, Boyadjian A, Allam N, Brasil-Neto JP (2012) Abnormal acute changes in upper limb muscle cortical representation areas in the patients with writer's cramp during co-activation of distal and proximal muscles. Acta Physiol (Oxf) 206:195–207 doi: 10.1111/j.1748-1716.2012.02451.x [PubMed: 22574750]

Tyc F, Boyadjian A, Devanne H (2005) Motor cortex plasticity induced by extensive training revealed by transcranial magnetic stimulation in human. Eur J Neurosci 21:259–266 doi: 10.1111/j.1460-9568.2004.03835.x [PubMed: 15654863]

van de Ruit M, Grey MJ (2016) The TMS Map Scales with Increased Stimulation Intensity and Muscle Activation. Brain Topogr 29:56–66 doi: 10.1007/s10548-015-0447-1 [PubMed: 26337508]

Vigano L, Fornia L, Rossi M, et al. (2019) Anatomo-functional characterisation of the human "hand-knob": A direct electrophysiological study. Cortex 113:239–254 doi: 10.1016/j.cortex.2018.12.011 [PubMed: 30708312]

Wassermann EM, McShane LM, Hallett M, Cohen LG (1992) Noninvasive mapping of muscle representations in human motor cortex. Electroencephalogr Clin Neurophysiol 85:1–8 doi: 10.1016/0168-5597(92)90094-r [PubMed: 1371738]

Wilson SA, Thickbroom GW, Mastaglia FL (1993) Transcranial magnetic stimulation mapping of the motor cortex in normal subjects. The representation of two intrinsic hand muscles. J Neurol Sci 118:134–144 doi: 10.1016/0022-510x(93)90102-5 [PubMed: 8229061]

Yousry TA, Schmid UD, Alkadhi H, Schmidt D, Peraud A, Buettner A, Winkler P (1997) Localization of the motor hand area to a knob on the precentral gyrus. A new landmark. Brain 120 (Pt 1):141–157 doi: 10.1093/brain/120.1.141 [PubMed: 9055804]

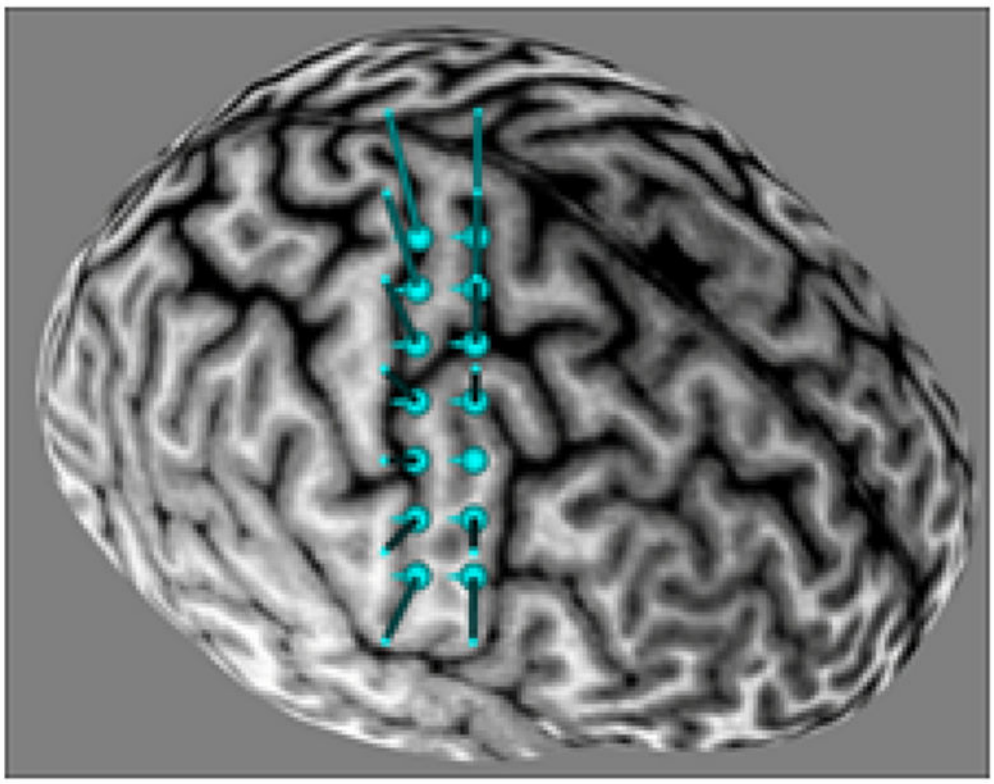

Site #	
1	2
3	4
5	6
7	8
9	10
11	12
13	14

Figure 1:

Location of stimulation sites, as viewed in Brainsight neuronavigation software

Using each participant's T1-weighted anatomical image and Brainsight software, stimulation targets were placed in a 7 × 2 grid pattern with 1 cm spacing, aligned over the right precentral gyrus. The grid was positioned parallel to and centered rostrocaudally over the precentral gyrus, and the middle row was aligned mediolaterally with the anatomical landmark known as the 'hand knob'. Curvature of the grid was adjusted to optimize placement of the stimulation targets on the cortical surface.

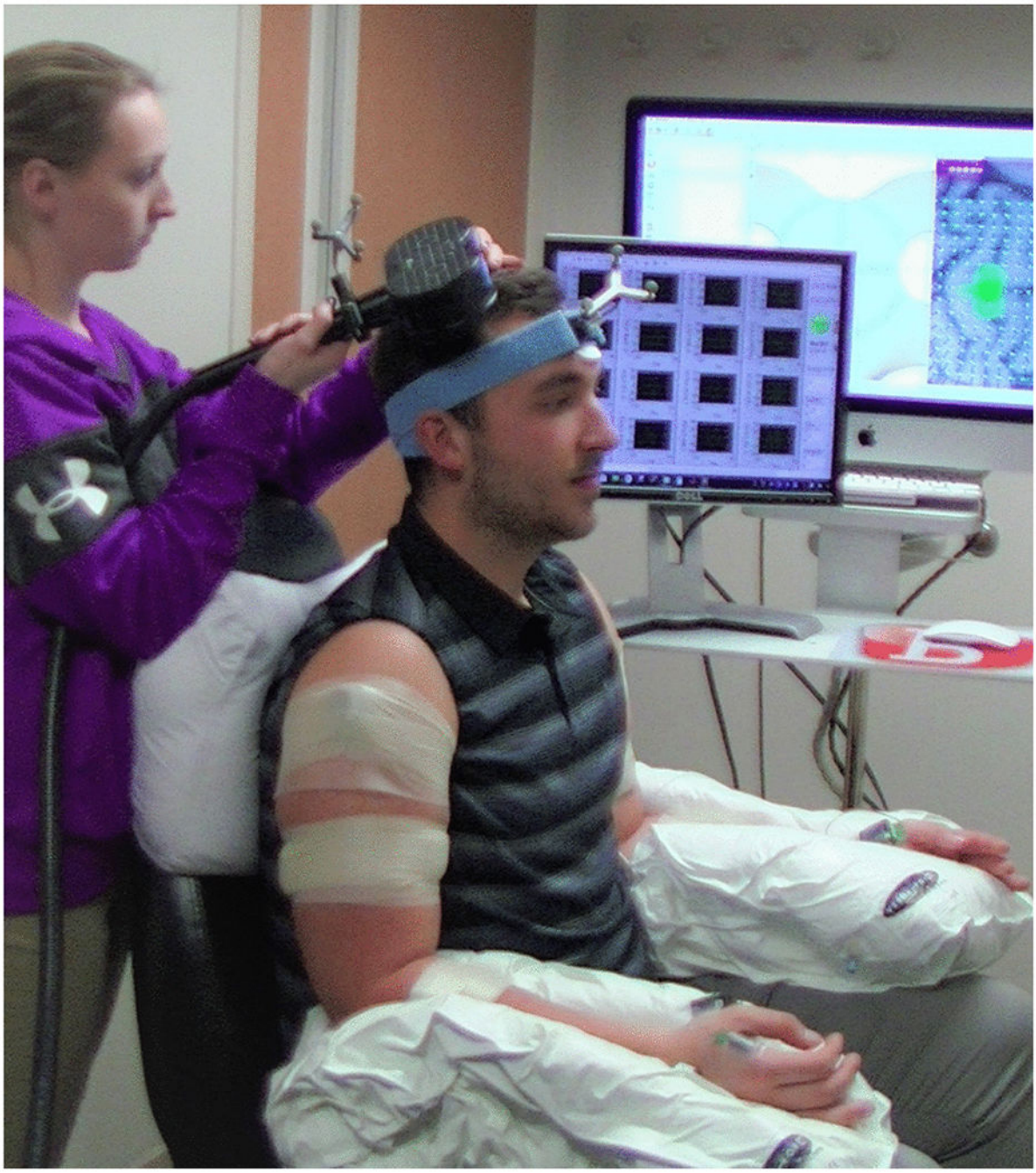

Figure 2:
Experimental setup and positioning
Participants were seated in a slightly reclined barber chair. Each arm was positioned using a Versaform vacuum molded pillow.

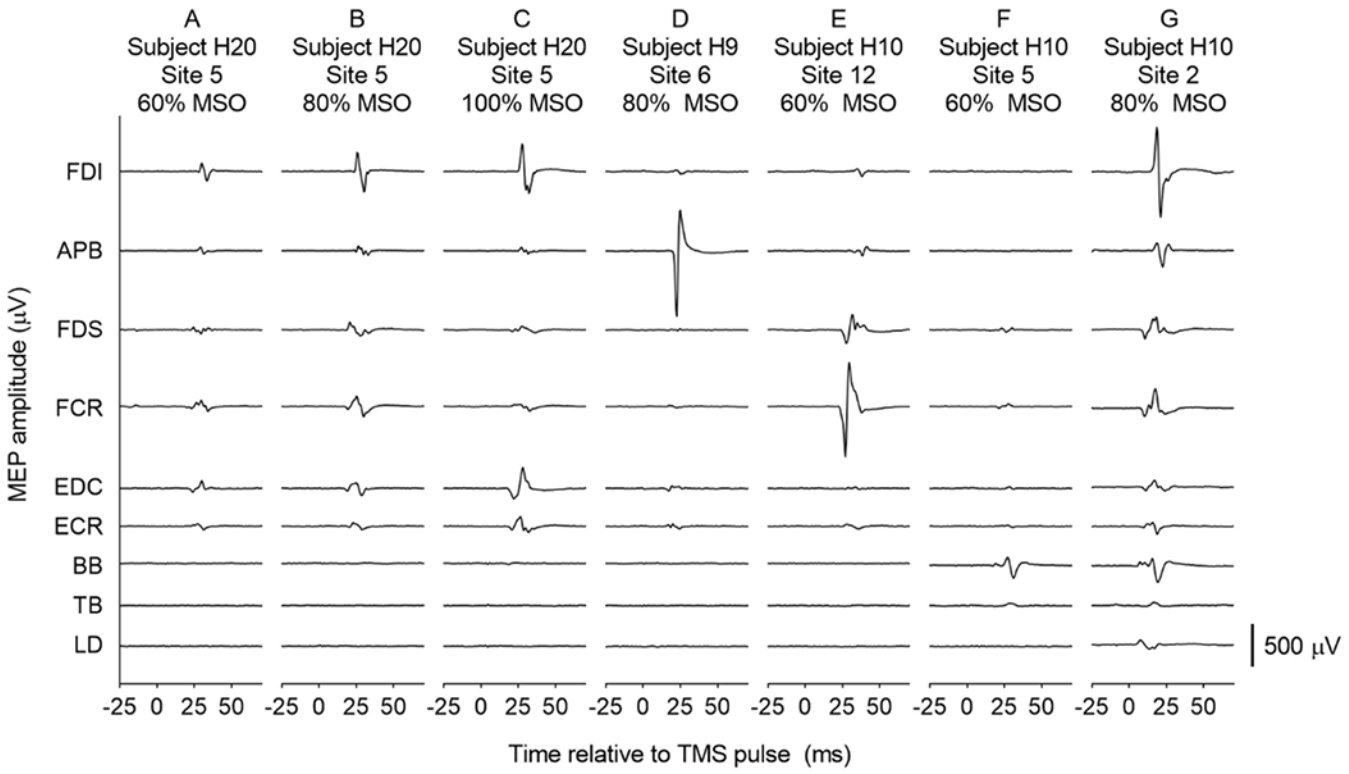

Figure 3:

Examples of raw MEPs

Electromyography recordings from 9 upper limb muscles, 25 ms before to 75 ms after a single TMS pulse was delivered to the contralateral primary motor cortex in individual participants. Panels A, B and C show a consistent coactivation pattern and increasing MEP amplitudes with increasing stimulus intensity in one participant. In different participants, Panel D shows a large MEP in only one muscle, and Panel E shows MEPs in two synergists, with minimal activation of any other muscles. Panel F demonstrates activation of a proximal muscle (BB) at submaximal intensity, with no MEPs in any distal muscles. As shown in Panel G, MEPs were sometimes observed in all 9 muscles, at a maximal or submaximal stimulus intensity. The y axis represents the difference in electrical potential across two parallel silver bars, 1 cm apart, over the middle of the muscle belly. Positive and negative directions of the y axis are not labeled, since the signal polarity is arbitrary, depending only on which end of the sensor is more distal when applied to the skin.

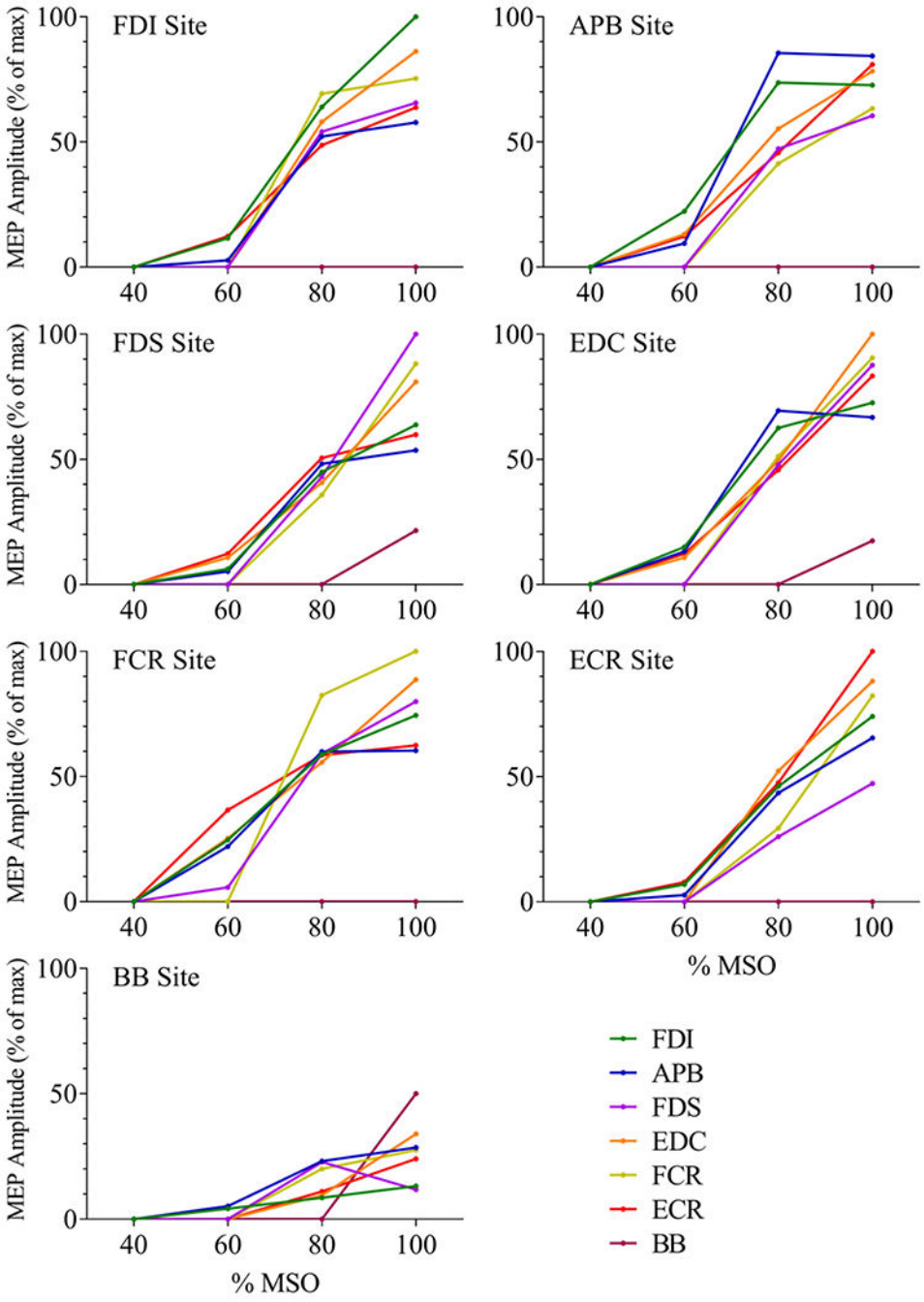

Figure 4:

Stimulus-response plots for each muscle's most responsive site

The group median MEP amplitude for each muscle is plotted across four stimulus intensities, for each muscle's most responsive cortical site. The site at which TMS elicited the largest average MEP in a given muscle was considered to be the muscle's most responsive site. For the BB muscle, MEPs were elicited in only 5 of the 10 participants, thus the median BB MEP amplitude at the BB most responsive site was only 50%.

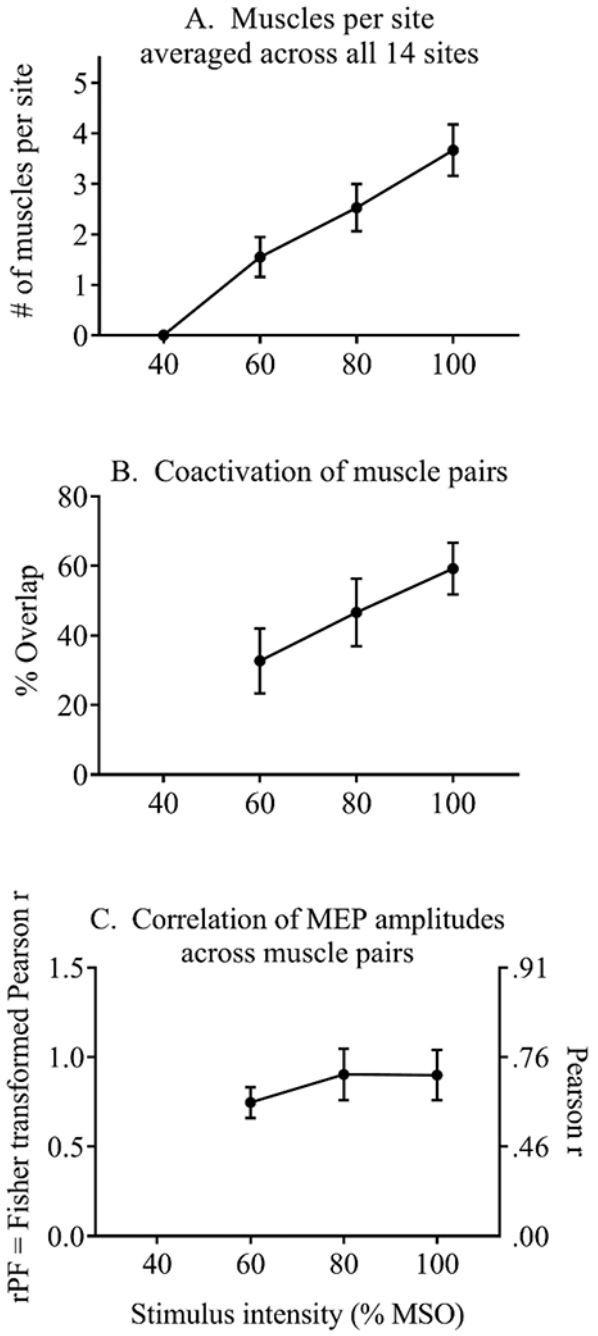

Figure 5:

Effect of stimulus intensity on the number of responsive muscles. coactivation, and correlation of MEP amplitudes

Mean ± 1 SE

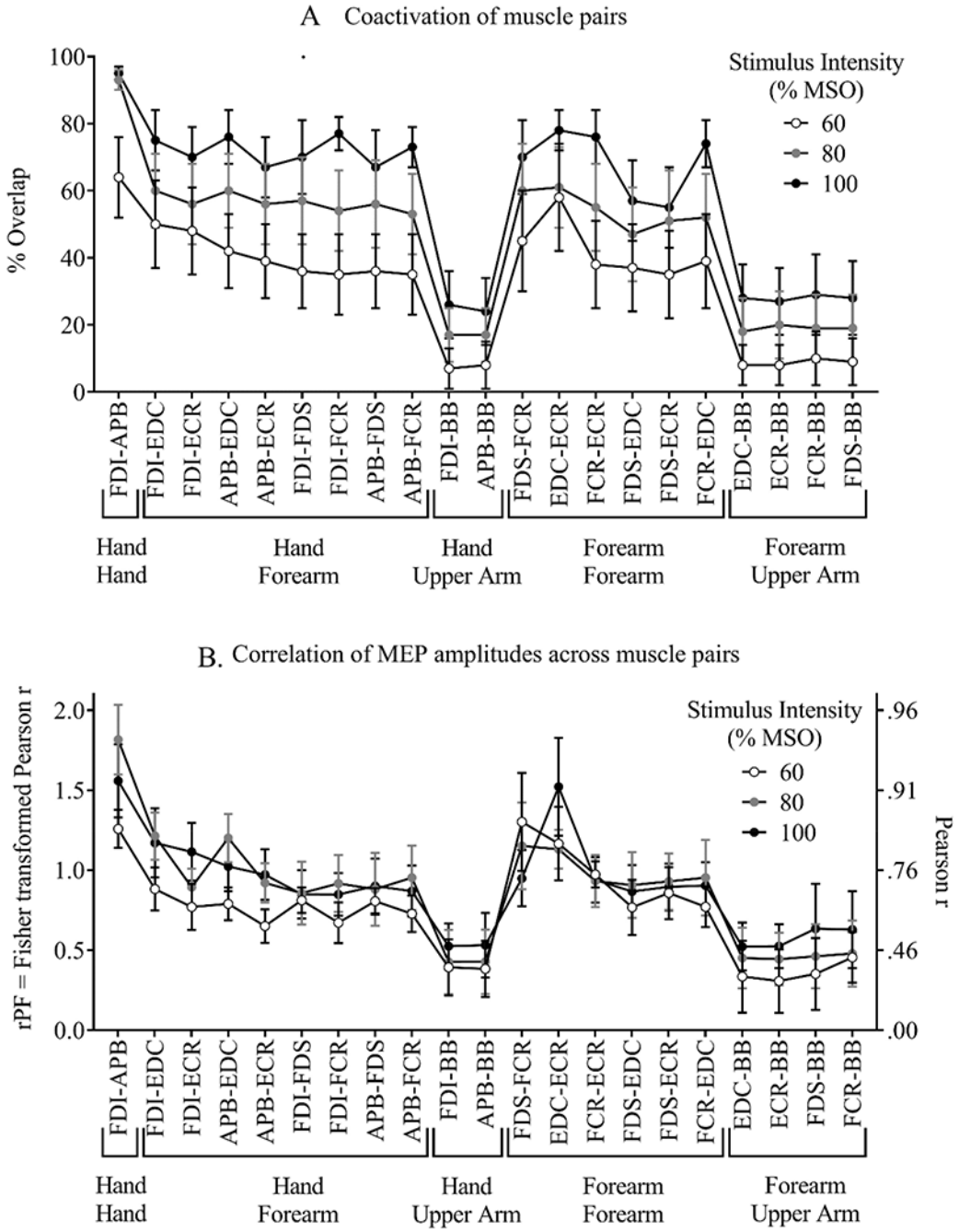

Figure 6:

Coactivation and correlation at each stimulus intensity for each muscle pair

Mean ± 1 SE, for each muscle pair and each stimulus intensity.

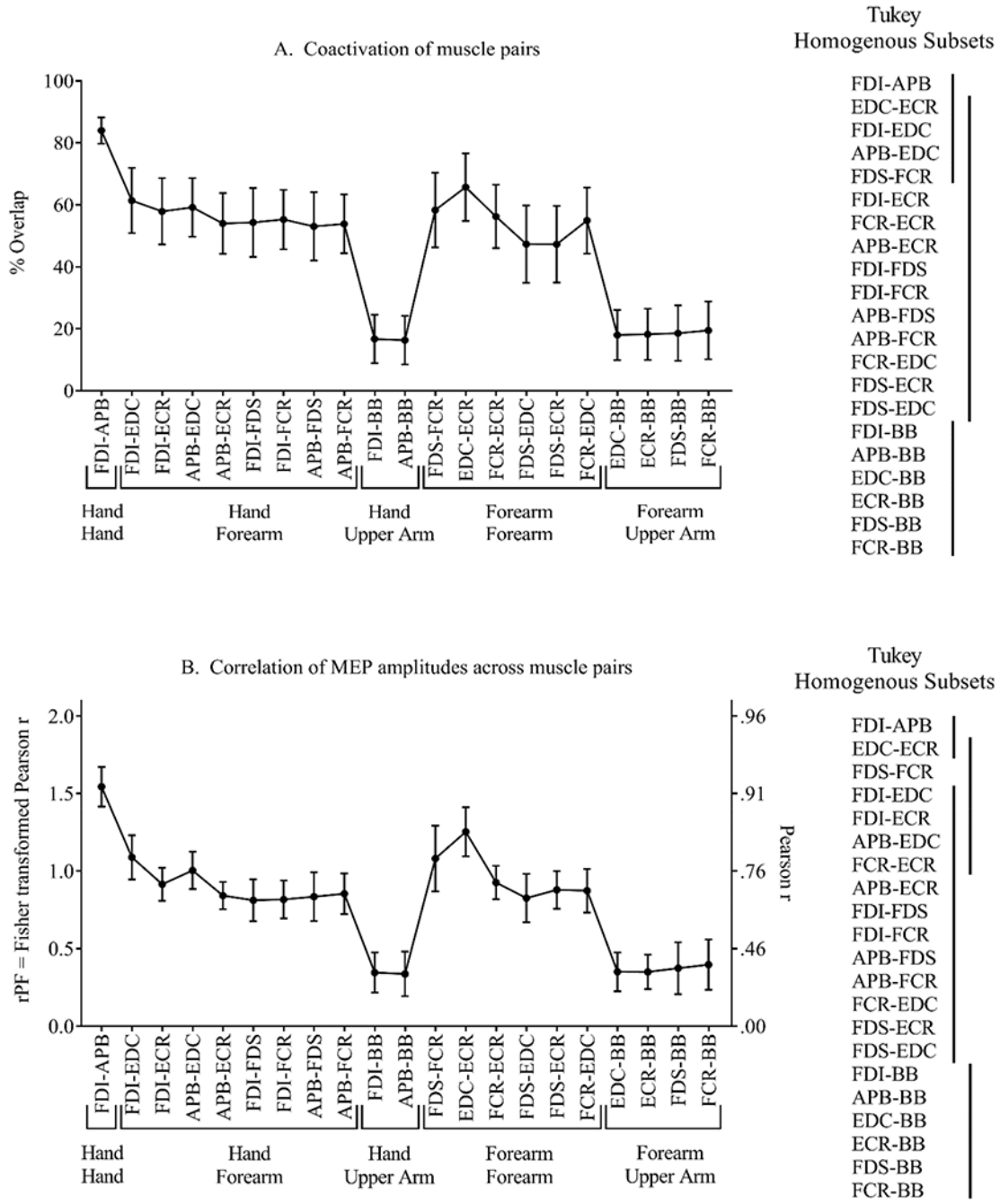

Figure 7:

Effect of muscle pair on coactivation and correlation

Mean ± 1 SE, for each muscle pair, averaged across the 3 stimulus intensities. Tukey post-hoc analysis identified 3 homogenous subsets for the coactivation variable (Panel A), and 4 homogenous subsets for the correlation variable (Panel B). Vertical lines indicate sets of muscle pairs that were statistically similar.

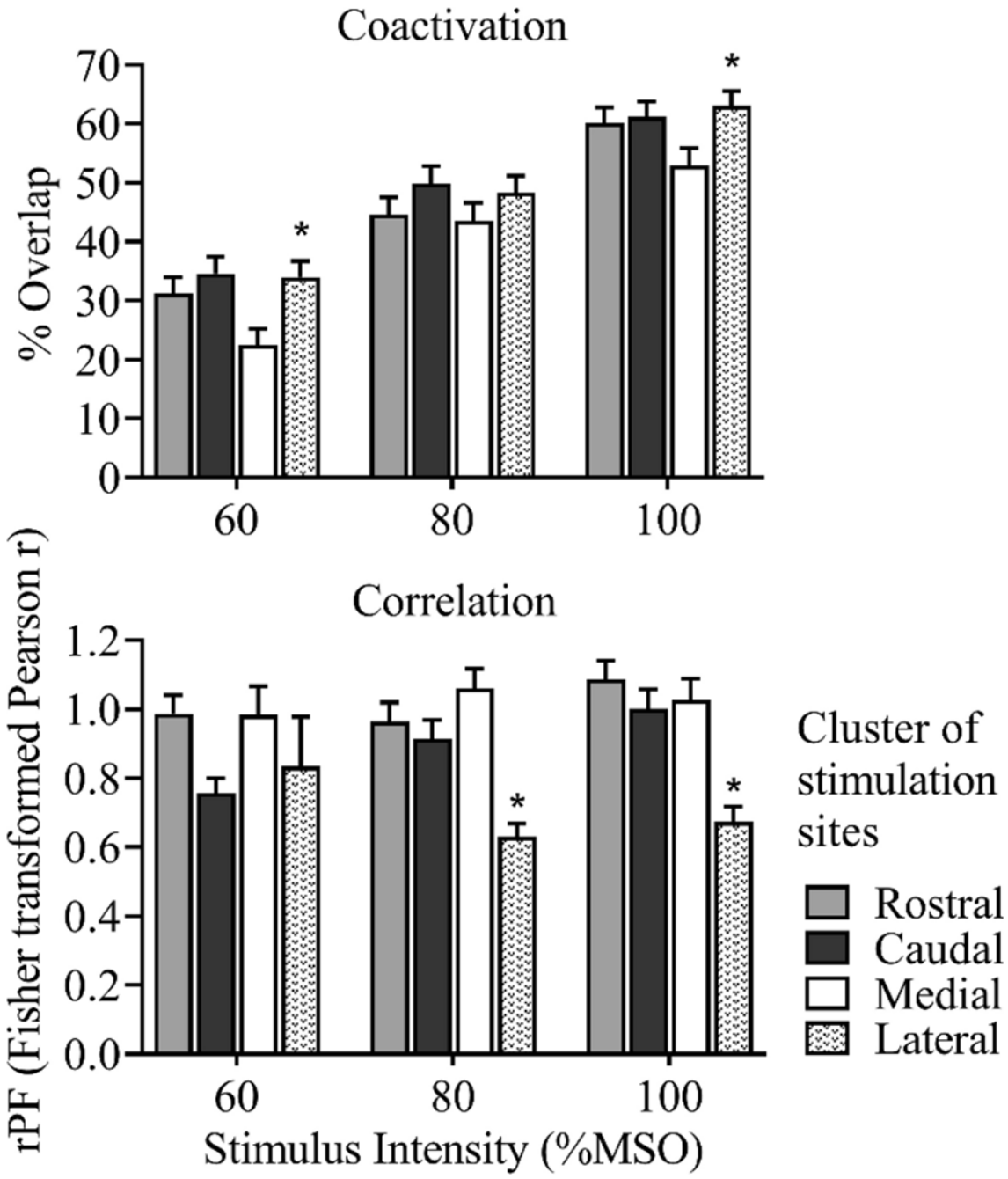

Figure 8:

Effect of site cluster on coactivation and correlation

Mean ± 1 SE, for each stimulus intensity, averaged across muscle pairs. Coactivation was greater in lateral sites compared to medial sites, at the 60% and 100% intensities. Correlations of MEP amplitudes were lower in lateral sites compared to medial sites, at the 80% and 100% intensities. * 2-way repeated measures ANOVA, main effect of site cluster, $p < 0.001$.

Table 1:

Area under the stimulus-response plot for each muscle at each cortical site

Values in the table represent the area under the stimulus-response plot. Mdn = Median value across the 10 participants. Each stimulus-response plot was created by plotting the average normalized MEP amplitude across the 4 intensities tested (40, 60, 80 and 100% MSO), as shown in Figure 4. Units of the area under the plot are % of maximal MEP multiplied by % MSO. For reference, if a given muscle's MEP amplitude at a given cortical site increased linearly from 0 at 40% MSO to 100% of the maximum MEP observed in that muscle at 100% MSO, the area under the plot would be 3000 (ie. 100% of maximum MEP multiplied by 60% MSO, divided by 2). In contrast, if a given muscle's MEP amplitude at a given cortical site was 0 at 40, 60 and 80% MSO and was 30% of its maximum MEP at 100% MSO, the area under the plot would be 300 (ie. 30% of maximum MEP multiplied by 20% MSO, divided by 2). n = the number of subjects from whom an MEP > 50 μV was elicited in the given muscle at the given cortical site, at any intensity. The most responsive site is defined as the site where the largest average MEP was elicited for the given muscle. See text for muscle name abbreviations.

Numbered Sites																		
Site	**FDI**		**APB**		**FDS**		**EDC**		**FCR**		**ECR**		**BB**		**TB**		**LD**	
	Mdn	**n**	**Mdn**	**n**	**Mdn**	**n**	**Mdn**	**n**	**Mdn**	**n**	**Mdn**	**n**	**Mdn**	**n**	**Mdn**	**n**	**Mdn**	**n**
1	0	1	0	0	0	1	0	2	0	2	0	2	0	1	0	1	0	1
2	0	2	0	1	0	2	0	2	0	2	0	2	0	1	0	2	0	1
3	124	6	33	5	139	5	485	6	116	5	294	5	0	4	0	2	0	1
4	159	5	106	6	179	5	563	6	267	5	0	4	0	4	0	2	0	1
5	1518	9	969	9	2004	7	2076	8	1983	8	1991	7	0	4	0	2	0	2
6	1645	9	1107	9	2085	7	1885	9	1765	8	1665	7	0	4	0	2	0	2
7	2687	9	1942	10	1576	8	2921	10	2146	9	2480	8	344	5	0	2	0	3
8	2697	9	1830	9	2327	8	2250	8	2290	9	1998	8	284	5	0	2	0	2
9	2241	10	2314	10	1237	8	1951	10	1819	10	1695	10	0	3	0	1	0	1
10	2049	10	2445	10	1605	7	2108	9	1417	9	1450	9	0	3	0	1	0	2
11	1119	10	1203	10	508	8	517	7	613	7	485	7	0	3	0	0	0	0
12	537	10	1135	10	722	6	454	6	598	6	0	4	0	1	0	0	0	0
13	0	3	0	4	0	2	0	3	0	2	0	3	0	0	0	0	0	0
14	0	4	0	4	0	3	0	3	0	2	0	2	0	0	0	0	0	0
Most responsive site for each muscle																		
Site	**FDI**		**APB**		**FDS**		**EDC**		**FCR**		**ECR**		**BB**		**TB**		**LD**	
	Mdn	**n**	**Mdn**	**n**	**Mdn**	**n**	**Mdn**	**n**	**Mdn**	**n**	**Mdn**	**n**	**Mdn**	**n**	**Mdn**	**n**	**Mdn**	**n**
FDI	2343	10	2323	10	1842	8	2492	10	2266	10	2273	9	0	4	0	1	0	2
APB	2886	10	2675	10	1680	8	2609	9	1925	10	2443	9	0	4	0	1	0	1
FDS	2047	9	1769	9	2430	9	2422	9	1956	9	2114	7	360	5	0	1	0	2
EDC	2423	10	2526	10	1795	8	2339	10	2078	10	2115	10	255	5	0	0	0	0
FCR	2648	10	2438	10	2263	9	2609	10	2846	10	2520	10	0	4	0	0	0	0
ECR	1777	10	1743	10	1001	8	2277	10	1227	10	2432	10	0	3	0	0	0	0

Numbered Sites																		
Site	FDI		APB		FDS		EDC		FCR		ECR		BB		TB		LD	
	Mdn	n	Mdn	n	Mdn	n	Mdn	n	Mdn	n	Mdn	n	Mdn	n	Mdn	n	Mdn	n
BB	663	5	1265	5	1062	5	926	5	1181	5	910	5	500	5	0	1	0	1
TB	0	1	0	1	0	1	0	1	0	1	0	1	0	1	0	1	0	0
LD	0	2	0	2	0	2	0	2	0	2	0	1	0	1	0	1	0	2